Published in final edited form as:
Bioelectrochemistry. 2010 August ; 79(1): 95–100. doi:10.1016/j.bioelechem.2009.12.007.

Gadolinium blocks membrane permeabilization induced by nanosecond electric pulses and reduces cell death

Franck M. André*, **Mikhail A. Rassokhin**, **Angela M. Bowman**, and **Andrei G. Pakhomov**
Frank Reidy Research Center for Bioelectrics, Old Dominion University, Norfolk, VA, USA

Abstract

It has been widely accepted that nanosecond electric pulses (nsEP) are distinguished from micro-and millisecond duration pulses by their ability to cause intracellular effects and cell death with reduced effects on the cell plasma membrane. However, we found that nsEP-induced cell death is most likely mediated by the plasma membrane disruption. We showed that nsEP can cause long-lasting (minutes) increase in plasma membrane electrical conductance and disrupt electrolyte balance, followed by water uptake, cell swelling and blebbing. These effects of plasma membrane permeabilization could be blocked by Gd^{3+} in a dose-dependent manner, with a threshold at sub-micromolar concentrations. Consequently, Gd^{3+} protected cells from nsEP-induced cell death, thereby pointing to plasma membrane permeabilization as a likely primary mechanism of lethal cell damage.

Keywords

Permeabilization; Plasma membrane; Cell death; Nanosecond electric pulses; Gadolinium

Introduction

Tissue ablation and tumor destruction are probably the most promising medical applications of high-voltage nsEP. This treatment induced apoptotic and necrotic death in various cancer cells in vitro, stimulated tumor regression in vivo, and were successfully employed to treat basal cell carcinoma in a human trial [1–3]. However, the primary target and cell mechanisms responsible for nsEP-induced cell death are not known, which hinders translation of this modality into clinical practice.

In early studies, nsEP were shown to have limited effects on the plasma membrane and target intracellular structures directly [4–7]. Indeed, dielectric breakdown of the plasma membrane, which is the best known effect of longer (micro- and millisecond range) electric pulses [8], was ruled out by the lack of immediate uptake of membrane integrity marker dyes [1,6,9] and nsEP-induced apoptosis was supposed to be independent from plasma membrane electroporation [1]. However, several publications showed that nsEP can charge plasma membrane and change the transmembrane potential [10,11], cause fast externalization of phosphatidylserine residues [9,12], induce plasma membrane permeabilization [11,13,14] and calcium influx through the plasma membrane [15].

*Corresponding author. Address: Frank Reidy Research Centre for Bioelectrics, 830 Southampton Ave., Suite 5100, Old Dominion University, Norfolk, VA 23510, USA. Tel: +1 757 297 0506. Fax: +1 757 314 2397., franckandre1@gmail.com.

Indeed, as predicted by electrical models and simulations, nsEP have effects on both intracellular structures and plasma membrane. Reducing the pulses duration results in decreased plasma membrane permeabilization and delayed propidium uptake with increased intracellular effects [1,13]. On the contrary increasing the pulse duration, the number of pulses or the electric field intensity results in faster uptake of membrane permeability markers and increases the percentage of permeabilized cells [11,16].

Nonetheless, recently it was reported that even a single 60 ns pulse at 12 kV/cm was enough to cause a profound and long-lasting (minutes) increase in membrane electrical conductance, accompanied by the loss of the membrane potential and permeabilization to small ions, but not to larger molecules such as propidium [17,18]. Likewise, simulation studies found that nsEP should open nanometer-size electropores both in the cell plasma membrane and organelles [19,20], and the existence of stable nanopores in the plasma membrane of nsEP-treated cells has been confirmed experimentally [21]. Furthermore, membrane permeabilization to small ions occurred at nsEP intensities significantly lower than the threshold for other known nsEP effects [22]. Therefore it is likely that plasma membrane permeabilization was missed by earlier studies due to the limits of the detection techniques used. Thereby suggesting that it could be a primary mechanism of other nsEP effects, including nsEP-induced cell death.

Should it be the case, then one might reasonably anticipate that chemical and physical agents that inhibit nsEP-induced plasma membrane permeabilization effect will also increase the survival of nsEP-treated cells. So far, among various chemical agents tested, only the lanthanide ions (Gd^{3+} and La^{3+}) were found to inhibit the nsEP-induced permeabilization, and, most likely, it was a direct effect on the membrane [17]. The lanthanides also prevented swelling and blebbing in severely exposed cells, which supported the idea that these necrotic manifestations could be caused by membrane disruption. However, potential effect of the lanthanides on cell survival after nsEP exposure has not been studied. Furthermore, lanthanides were only tested at high (millimolar) concentrations, which increased the likelihood of non-specific mechanisms of their action.

The goals of the present study were (1) to explore modulation of membrane effects of nsEP by Gd^{3+} in a wide range of concentrations, (2) to test if Gd^{3+} can also increase cell survival after nsEP exposure. If inhibition of nsEP-induced membrane permeabilization by Gd^{3+} also improves cell survival, this observation would point at the impairment of the plasma membrane barrier function as a likely primary mechanism responsible for nsEP-induced cell death.

Materials and methods

Cell cultures

Jurkat clone E6-1 (human T cell leukemia) and GH3 cells (murine pituitary) were obtained from American Type Culture Collection (Manassas, VA). Cells were maintained in the logarithmic stage of growth at 37 °C with 5 % CO_2 in air and used at passages 3 to 15. GH3 cells were cultured in Ham's F12K medium supplemented with 2.5 % fetal bovine serum (FBS) and 15 % horse serum. Jurkat cells were propagated in RPMI-1640 medium with 10 % FBS and 2 mM L-glutamine. The growth media also contained 100 IU/ml penicillin/streptomycin. The media and its components were purchased from Mediatech Cellgro (Herndon, VA) except for the animal sera (Atlanta Biologicals, Norcross, GA). For patch clamp and imaging experiments, cells were allowed a minimum of one day to adhere to glass coverslips covered with poly-L-lysine (Sigma-Aldrich, St. Louis, MO).

Chemicals and solutions

Cells were exposed to nsEP in a buffer composed of (hereinafter in mM) 135 NaCl, 5 KCl, 2 $MgCl_2$, 10 HEPES, X $GdCl_3$, and 10 glucose (pH 7.4), where X was varied from 0 to 1 mM. To assess plasma membrane integrity by dye exclusion, this buffer was supplemented with a membrane-impermeable fluorescent DNA stain, propidium iodide (PI, 10 or 30 μg/ml). For patch clamp experiments, recording pipette was filled with 140 KCl, 5 K-EGTA, 4 $MgCl_2$, and 10 HEPES (pH 7.2). The osmolality of the solutions was between 290 and 310 mOsm, as measured with a freezing point microosmometer (Advanced Instruments, Inc., Norwood, MA, USA). All chemicals were purchased from Sigma–Aldrich.

Cell imaging

Cells on a coverslip were transferred into a glass-bottomed chamber (Warner Instruments, Hamden, CT) mounted on an IX71 microscope configured with an FluoView 300 confocal laser scanning system (Olympus America Inc., Center Valley, PA). Differential interference contrast (DIC) and fluorescence images of cells were obtained with a 40x, 0.75 NA no-immersion objective. The images were taken as a time series, starting before nsEP exposure and continuing for several minutes after it. The effect of Gd^{3+} was identified by comparing morphological changes and propidium uptake in cells that were held at different Gd^{3+} concentrations while receiving the same nsEP treatments. Cell images were quantified off-line with MetaMorph v. 7.5 (MDS, Foster City, CA).

Patch clamp

We used the same setup as for the cell imaging, but the chamber was continually superfused with Gd^{3+}-free bath buffer at a rate of 0.9 ml/min. Unlike the imaging experiments, Gd^{3+} -containing buffer was applied 40–50 sec after nsEP exposure, at 0.15 ml/min locally to the selected cell using 28G MicroFil needle (World Precision Instruments, Sarasota, FL). These experiments were intended to check if Gd^{3+} can revert nsEP-induced changes in the plasma membrane electrical conductance.

Recording pipettes were pulled from borosilicate glass (BF150-86-10, Sutter Instrument, Novato, CA) to a tip resistance of 1.5–3 MΩ. Seal and access resistance values were between 2–10 GΩ and 10–20 MΩ, respectively. Whole-cell currents were probed every 5–10 s by applying 120 ms voltage steps in 10 mV increments, from −100 to +40 mV; holding potential between the sweeps was −80 mV. Currents were measured as mean value at the plateau level, 50–110 ms after the start of the step. Passive membrane resistance (R_m) was defined as $\Delta V/\Delta I$ in a range that contained no visible voltage-activated currents, from −80 to −70 mV.

The data were collected using a Multiclamp 700B amplifier, Digidata 1322A A–D converter, and pCLAMP 10 software (MDS). Command voltages were corrected for the junction potential of −4.2 mV.

NsEP exposure

Two different systems were employed for exposure of individual cells on coverslips (patch clamp and microscopy measurements) and for bulk exposure of cell population in electroporation cuvettes (cell survival studies).

The setup for individual cell exposure was previously described [21]. In brief, 60 or 600 ns pulses were generated in a transmission line-type circuit and delivered to a selected cell with a pair of tungsten rod electrodes (0.1 mm diameter, 0.16 mm gap). These electrodes were positioned precisely 50 μm above the coverslip surface so that the selected cell was in the middle of the gap between their tips. The E-field at the cell location between the electrodes

was determined by 3D simulations with a finite element Maxwell equations solver Amaze 3D (Field Precision, Albuquerque, NM).

For cell survival studies, 2×10^6 cells suspended in 420 μl of bath buffer (with or without Gd^{3+}) were placed in a 2 mm gap electroporation cuvette (Biosmith Biotech, San Diego, CA). 60 ns pulses at 2 Hz were produced by a Blumlein line generator; the E-field in the cuvette was calculated by dividing the applied voltage by the gap distance. Five minutes after exposure, cells were diluted 5x by the same buffer that was used for exposure and incubated for 0.25 to 5 h until cell viability measurements. All nsEP exposures and subsequent manipulations (except MTT assay, see below) were performed at a room temperature of 22–24 °C.

Cell viability assays

Propidium exclusion, as measured by flow cytometry 0.25 to 5 h post nsEP exposure, served as a principal index of cell survival. PI was added to an aliquot of exposed cells five minutes prior to measurements to a final concentration of 10 μg/ml. A total of 10,000 cells per sample were checked for propidium uptake using a FACSARIA flow cytometer (Becton–Dickinson, Franklin Lakes, NJ). Cells that showed no propidium fluorescence (488 nm excitation, 695/40 nm emission) were defined as viable. The number of viable cells in each group was expressed as a percentage to the respective parallel control sample (sham exposure and no Gd^{3+}).

Of note, electroporation of cells by nsEP could cause modest immediate uptake of propidium (see fluorescent microscopy data below), which did not necessarily indicate cell death (the membrane could potentially re-seal later on [21]. In contrast, intense propidium uptake at long time intervals post exposure was regarded as permanent membrane damage and cell death.

In addition, cell viability was assessed by the activity of mitochondrial dehydrogenases, as measured by conversion of MTT reagent into blue formazan (CellQuanti-MTT cell viability assay kit, BioAssay Systems, Hayward, CA). One hour after exposure, 15 μl of MTT reagent and PI (to 10 μg/ml) were added to 100 μl aliquots of cell suspension in a 96-well plate, and the plate was incubated for 3 h (37 °C, 5% CO_2). Then, 85 μl of MTT solubilization buffer were added to each well and left overnight in the dark at room temperature. The absorbance at 570 nm and PI fluorescence (excitation: 485/20 nm, emission: 590/35 nm) were read the next morning with Synergy 2 microplate reader (BioTEK, Winooski, VT). In order to ensure the consistency of the data with the previous flow cytometry measurements, the same samples in the 96-well plates were checked for propidium uptake one hour after the exposure.

Statistical analysis

Results are expressed as means ± s.e.. Statistical analysis was performed by Student's paired t test, or by one way ANOVA followed by Holm-Sidak t-test for multiple comparisons versus control.

Results

Gd^{3+} restores Rm in nsEP-exposed cells

A profound, long-lasting decrease of Rm was uniformly observed in different mammalian cell lines subjected to relatively mild nsEP exposure [17,18,22]. In healthy undisturbed Jurkat cells, Rm values were typically between 2 and 10 GΩ. A single 60 ns pulse at 8 kV/cm instantly decreased Rm 10 to 100 fold (Fig. 1), and also induced characteristic inward rectification [21]. Addition of Gd^{3+} efficiently restored Rm in a concentration-dependent manner. Gd^{3+} effect became significant at concentration as low as 0.1 μM, and reached saturation at 1 μM. At the highest concentrations tested, Rm restoration was practically instant (data not shown).

These results point to a direct effect of Gd^{3+} on the cell membrane, rather than mediated by other mechanisms, and support the earlier findings [17].

Of note, Gd^{3+} restored Rm, but not the original shape of the current-voltage (I–V) curve (Fig. 1, insets). This can likely be explained by a concurrent effect of nsEP and/or Gd^{3+} on voltage-activated K^+ channels in Jurkat cells, which is beyond the scope of this study.

Gd^{3+} attenuates nsEP-induced cytophysiological changes

More intense nsEP treatments (e.g., a train of 100 pulses, 60 ns, 12 kV/cm) caused fast changes in the cell shape and volume, along with cytoplasm granulation (Fig. 2, A). Within seconds after exposure, cell started swelling and developed large and often multiple blebs, with no signs of recovery within the observation period (up to 10 min). Interestingly, this massive water uptake due to permeabilization of the cell plasma membrane was accompanied by only a modest (if any), gradual uptake of propidium (Fig. 2, B(1)). In contrast, a chemical membrane poration with digitonin caused an instantaneous and 40 times more intense uptake of the dye (Fig. 2, B (3)). These findings are consistent with previous reports that nsEP-opened membrane pores are permeable to small inorganic ions, but probably are too small to allow the passage of the larger propidium cation [17, 21].

Fig 2 also shows that the presence of Gd^{3+} in the bath buffer, at tested concentrations of 10 and 1,000 μM, effectively prevented formation of local blebs and significantly reduced cell swelling (as judged from the change of the visible cell cross-section). Gd^{3+} also attenuated propidium uptake ($p<0.01$), to the same extent by 10 (Fig. 2, B(2)) and 100 μM concentrations (the latter data not shown), although it did not block the dye uptake entirely. Overall, the cytophysiological findings were consistent with the concept of plasma membrane nanoporation by nsEP [21], and confirmed that Gd^{3+} attenuates this effect.

Gd^{3+} increases cell survival after nsEP exposure

The fraction of Jurkat cells that excluded propidium gradually decreased within the first hour after an intense nsEP exposure (10 or 30 pulses, 60 ns, 20 kV/cm), and then reached a plateau (Fig. 3, A). The presence of 30 μM Gd^{3+} in the exposure and incubation medium profoundly increased cell survival ($p < 0.01$ for up to 4 h); however, the protective effect of Gd^{3+} gradually decreased with time due to the toxicity of this ion [23]. Indeed, Fig. 3, A shows gradual reduction of cell survival with time in cells that were incubated with Gd^{3+} without nsEP exposure.

For more detailed experiments we chose a time point 1 h after exposure, when the nsEP effect already reached maximum, but cell death due to Gd^{3+} toxicity was minimal. Fig 3, B shows that the threshold for the protective effect of Gd^{3+} became significant at a concentration of 0.1 μM, same as the threshold found above by patch-clamp measurements. The protective effect of Gd^{3+} could be seen up to 30–60 μM (a separate set of experiments, Fig. 3, B(ii)). Furthermore, at 30 μM and higher concentrations, the cell death rate was apparently determined by Gd^{3+} concentration only, irrespective of the fact whether the cells were exposed to nsEP or not.

These findings were corroborated by the MTT viability assay. The presence of Gd^{3+} (10 or 30 μM) increased viability of nsEP-exposed Jurkat cells (20pulses, 60 ns, 20 kV/cm) by 43% and 30%, respectively (the lower efficiency of the higher Gd^{3+} concentration was likely a result of suppression of mitochondrial activity due to Gd^{3+} toxicity). Concurrent measurement of propidium uptake using the microplate reader yielded results similar to the flow cytometry, namely, a 45% and 53% decrease of propidium uptake when Gd^{3+} was present at 10 and 30 μM, respectively.

Discussion

For the first time, our study demonstrated that Gd^{3+} ions, even in sub-micromolar concentrations, can weaken or revert electropermeabilization of the plasma membrane by nsEP. Concurrently, we found that Gd^{3+} increased survival of nsEP-exposed cells, thereby suggesting that the cell death after nsEP exposure is a consequence of the plasma membrane disruption. Internal effects of the Gd^{3+} are possible but are very unlikely to be responsible for the increased survival we observed. Indeed it has been shown that Gd^{3+} immediately binds to the plasma membrane lipids and proteins whereas 25 minutes later only a fraction (around $1/60^{th}$) of Gd^{3+} was able to diffuse through the plasma membrane [24]. Moreover, the link between plasma membrane permeabilization and cell death is strengthened by the fact that the threshold for Gd^{3+} effect is the same (about 0.1 μM) for both plasma membrane protection and cell death prevention. It would be expected to be 60 times higher if intracellular membranes protection was involved. This conclusion contradicts multiple earlier studies that suggested direct intracellular effects of nsEP as the reason for lethal cell damages [1,5,25]. However, these studies relied on the lack of immediate propidium uptake by nsEP-treated cells to conclude that the plasma membrane is not affected, and did not consider that it could be permeabilized selectively to smaller ions. Later studies clearly demonstrated such selective permeabilization, independently by both electrophysiological and imaging methods [17,21,22], so the leading role of the plasma membrane disruption in the nsEP-induced cell death is not surprising. On the other hand, our data do not exclude possible activation of classic ion channels (e.g., stretch-activated channels [26–28] and volume-sensitive Cl^- channels [26,29,30]), as well as involvement of cell membrane-independent mechanisms of cell damage.

The likely scenario of cell death induction by nsEP can simplistically be presented as a following sequence: (1) Formation of nanopores in plasma membrane by nsEP (by either dielectric breakdown, or oxidative damage, or deformation stress [31]. (2) Influx of Na^+ into the cell through nanopores, down the concentration and voltage gradients. (3) Na^+ influx is followed by osmotically obliged water, causing excessive hydration of larger, nanopore-impermeable molecules, cell swelling and blebbing. (4) Membrane potential shifts toward zero; transmembrane gradients of K^+ and Cl^- decrease due to activation of respective classic ion channels. (5) Na^+, K^+-ATPase and possibly other pumps are activated in order to restore the transmembrane ion balances; however, this effort will only be successful if pores reseal fast and if the cell has sufficient ATP supply. (6). Breaking of nanopores into larger pores due to excessive swelling, and/or exhaustion of ATP supply may trigger necrotic or apoptotic cell death.

Lanthanides are known to block multiple types of ion channels, including voltage-gated calcium channels, stretch-activated channels, several ionotropic and metabotropic ligand-gated channels; they can also inhibit Ca^{2+}- and Mg^{2+}-ATPases and Na^+/Ca^{2+} exchanger [32–35]. The mechanism of the action of lanthanide ions is not completely understood, but it appears to be related to the similarity of their cationic radii to the size of Ca^{2+} ions [32]. Recently, it was also demonstrated that Gd^{3+} can bind directly to the lipid bilayer to create lateral compression and stabilize the membrane [24,36], which could mediate its effects on ion channels. In fact, both the contemplated mechanisms could be as well applicable to blockage of nanopore formation and/or their resealing. Understanding of the exact mechanisms leading to cell death following nsEP exposure will help to explain differential sensitivity of mammalian cells to this factor and promote the development of nsEP medical applications.

Acknowledgments

We would like to thank Dr. S. Xiao for calculating E-field distribution in the individual cell exposures. This work was supported by NIH grant R01CA125482 from the National Cancer Institute.

References

1. Beebe SJ, Fox PM, Rec LJ, Willis EL, Schoenbach KH. Nanosecond, high-intensity pulsed electric fields induce apoptosis in human cells. FASEB J 2003;17:1493–1495. [PubMed: 12824299]
2. Garon EB, Sawcer D, Vernier PT, Tang T, Sun Y, Marcu L, Gundersen MA, Koeffler HP. In vitro and in vivo evaluation and a case report of intense nanosecond pulsed electric field as a local therapy for human malignancies. Int J Cancer 2007;121:675–682. [PubMed: 17417774]
3. Nuccitelli R, Chen X, Pakhomov AG, Baldwin WH, Sheikh S, Pomicter JL, Ren W, Osgood C, Swanson RJ, Kolb JF, Beebe SJ, Schoenbach KH. A new pulsed electric field therapy for melanoma disrupts the tumor's blood supply and causes complete remission without recurrence. Int J Cancer 2009;125:438–445. [PubMed: 19408306]
4. Schoenbach KH, Beebe SJ, Buescher ES. Intracellular effect of ultrashort electrical pulses. Bioelectromagnetics 2001;22:440–448. [PubMed: 11536285]
5. Stacey M, Stickley J, Fox P, Statler V, Schoenbach K, Beebe SJ, Buescher S. Differential effects in cells exposed to ultra-short, high intensity electric fields: cell survival, DNA damage, and cell cycle analysis. Mutat Res 2003;542:65–75. [PubMed: 14644355]
6. Vernier PT, Sun Y, Marcu L, Salemi S, Craft CM, Gundersen MA. Calcium bursts induced by nanosecond electric pulses. Biochem Biophys Res Commun 2003;310:286–295. [PubMed: 14521908]
7. Tekle E, Oubrahim H, Dzekunov SM, Kolb JF, Schoenbach KH, Chock PB. Selective field effects on intracellular vacuoles and vesicle membranes with nanosecond electric pulses. Biophys J 2005;89:274–284. [PubMed: 15821165]
8. Neumann, E.; Sowers, AE.; Jordan, CA. Electroporation and Electrofusion in Cell Biology. Plenum; New York: 1989.
9. Vernier PT, Sun Y, Marcu L, Craft CM, Gundersen MA. Nanoelectropulse-induced phosphatidylserine translocation. Biophys J 2004;86:4040–4048. [PubMed: 15189899]
10. Frey W, White JA, Price RO, Blackmore PF, Joshi RP, Nuccitelli R, Beebe SJ, Schoenbach KH, Kolb JF. Plasma membrane voltage changes during nanosecond pulsed electric field exposure. Biophys J 2006;90:3608–3615. [PubMed: 16513782]
11. Hair PS, Schoenbach KH, Buescher ES. Sub-microsecond, intense pulsed electric field applications to cells show specificity of effects. Bioelectrochemistry 2003;61:65–72. [PubMed: 14642911]
12. Vernier PT, Sun Y, Marcu L, Salem S, Craft CM, Gundersen MA. Calcium bursts induced by nanosecond electric pulses. Biochemical and Biophysical Research Communications 2003;310:286–295. [PubMed: 14521908]
13. Deng J, Schoenbach KH, Buescher ES, Hair PS, Fox PM, Beebe SJ. The effects of intense submicrosecond electrical pulses on cells. Biophys J 2003;84:2709–2714. [PubMed: 12668479]
14. Pliquett U, Joshi RP, Sridhara V, Schoenbach KH. High electrical field effects on cell membranes. Bioelectrochemistry 2007;70:275–282. [PubMed: 17123870]
15. Vernier PT, Sun Y, Chen MT, Gundersen MA, Craviso GL. Nanosecond electric pulse-induced calcium entry into chromaffin cells. Bioelectrochemistry 2008;73:1–4. [PubMed: 18407807]
16. Beebe SJ, Fox PM, Rec LJ, Somers K, Stark RH, Schoenbach KH. Nanosecond Pulsed Electric Field (nspef) Effects on Cells and Tissues: Apoptosis Induction and Tumor Growth Inhibition. IEEE Trans Plasma Sci 2002;30:286–292.
17. Pakhomov, AG.; Shevin, R.; White, JA.; Kolb, JF.; Pakhomova, ON.; Joshi, RP.; Schoenbach, KH. Arch Biochem Biophys. Vol. 465. 2007. Membrane permeabilization and cell damage by ultrashort electric field shocks; p. 109-118.
18. Pakhomov AG, Kolb JF, White JA, Joshi RP, Xiao S, Schoenbach KH. Long-lasting plasma membrane permeabilization in mammalian cells by nanosecond pulsed electric field (nsPEF). Bioelectromagnetics 2007;28:655–663. [PubMed: 17654532]
19. Gowrishankar TR, Weaver JC. Electrical behavior and pore accumulation in a multicellular model for conventional and supra-electroporation. Biochem Biophys Res Commun 2006;349:643–653. [PubMed: 16959217]
20. Hu Q, Joshi RP, Schoenbach KH. Simulations of nanopore formation and phosphatidylserine externalization in lipid membranes subjected to a high-intensity, ultrashort electric pulse. Phys Rev E Stat Nonlin Soft Matter Phys 2005;72:031902. [PubMed: 16241477]

21. Pakhomov AG, Bowman AM, Ibey BL, Andre FM, Pakhomova ON, Schoenbach KH. Lipid nanopores can form a stable, ion channel-like conduction pathway in cell membrane. Biochem Biophys Res Commun 2009;385:181–186. [PubMed: 19450553]
22. Ibey BL, Xiao S, Schoenbach KH, Murphy MR, Pakhomov AG. Plasma membrane permeabilization by 60- and 600-ns electric pulses is determined by the absorbed dose. Bioelectromagnetics 2009;30:92–99. [PubMed: 18839412]
23. Mizgerd JP, Molina RM, Stearns RC, Brain JD, Warner AE. Gadolinium induces macrophage apoptosis. J Leukoc Biol 1996;59:189–195. [PubMed: 8603991]
24. Cheng Y, Yao H, Lin H, Lu J, Li R, Wang K. The events relating to lanthanide ions enhanced permeability of human erythrocyte membrane: binding, conformational change, phase transition, perforation and ion transport. Chem Biol Interact 1999;121:267–289. [PubMed: 10462058]
25. Hall EH, Schoenbach KH, Beebe SJ. Nanosecond pulsed electric fields induce apoptosis in p53-wildtype and p53-null HCT116 colon carcinoma cells. Apoptosis 2007;12:1721–1731. [PubMed: 17520193]
26. Numata T, Shimizu T, Okada Y. TRPM7 is a stretch- and swelling-activated cation channel involved in volume regulation in human epithelial cells. Am J Physiol Cell Physiol 2007;292:C460–467. [PubMed: 16943238]
27. Pedersen SF, Owsianik G, Nilius B. TRP channels: an overview. Cell Calcium 2005;38:233–252. [PubMed: 16098585]
28. Clapham DE. TRP channels as cellular sensors. Nature 2003;426:517–524. [PubMed: 14654832]
29. Decher N, Lang HJ, Nilius B, Bruggemann A, Busch AE, Steinmeyer K. DCPIB is a novel selective blocker of I(Cl,swell) and prevents swelling-induced shortening of guinea-pig atrial action potential duration. Br J Pharmacol 2001;134:1467–1479. [PubMed: 11724753]
30. Okada Y, Shimizu T, Maeno E, Tanabe S, Wang X, Takahashi N. Volume-sensitive chloride channels involved in apoptotic volume decrease and cell death. J Membr Biol 2006;209:21–29. [PubMed: 16685598]
31. Sukhorukov VL, Mussauer H, Zimmermann U. The effect of electrical deformation forces on the electropermeabilization of erythrocyte membranes in low- and high-conductivity media. J Membr Biol 1998;163:235–245. [PubMed: 9625780]
32. Palasz A, Czekaj P. Toxicological and cytophysiological aspects of lanthanides action. Acta Biochim Pol 2000;47:1107–1114. [PubMed: 11996100]
33. Iwamoto T, Shigekawa M. Differential inhibition of Na+/Ca2+ exchanger isoforms by divalent cations and isothiourea derivative. Am J Physiol 1998;275:C423–430. [PubMed: 9688596]
34. Hamill OP, McBride DW Jr. The pharmacology of mechanogated membrane ion channels. Pharmacol Rev 1996;48:231–252. [PubMed: 8804105]
35. Lipski J, Park TI, Li D, Lee SC, Trevarton AJ, Chung KK, Freestone PS, Bai JZ. Involvement of TRP-like channels in the acute ischemic response of hippocampal CA1 neurons in brain slices. Brain Res 2006;1077:187–199. [PubMed: 16483552]
36. Tanaka T, Li SJ, Kinoshita K, Yamazaki M. La(3+) stabilizes the hexagonal II (H(II)) phase in phosphatidylethanolamine membranes. Biochim Biophys Acta 2001;1515:189–201. [PubMed: 11718674]

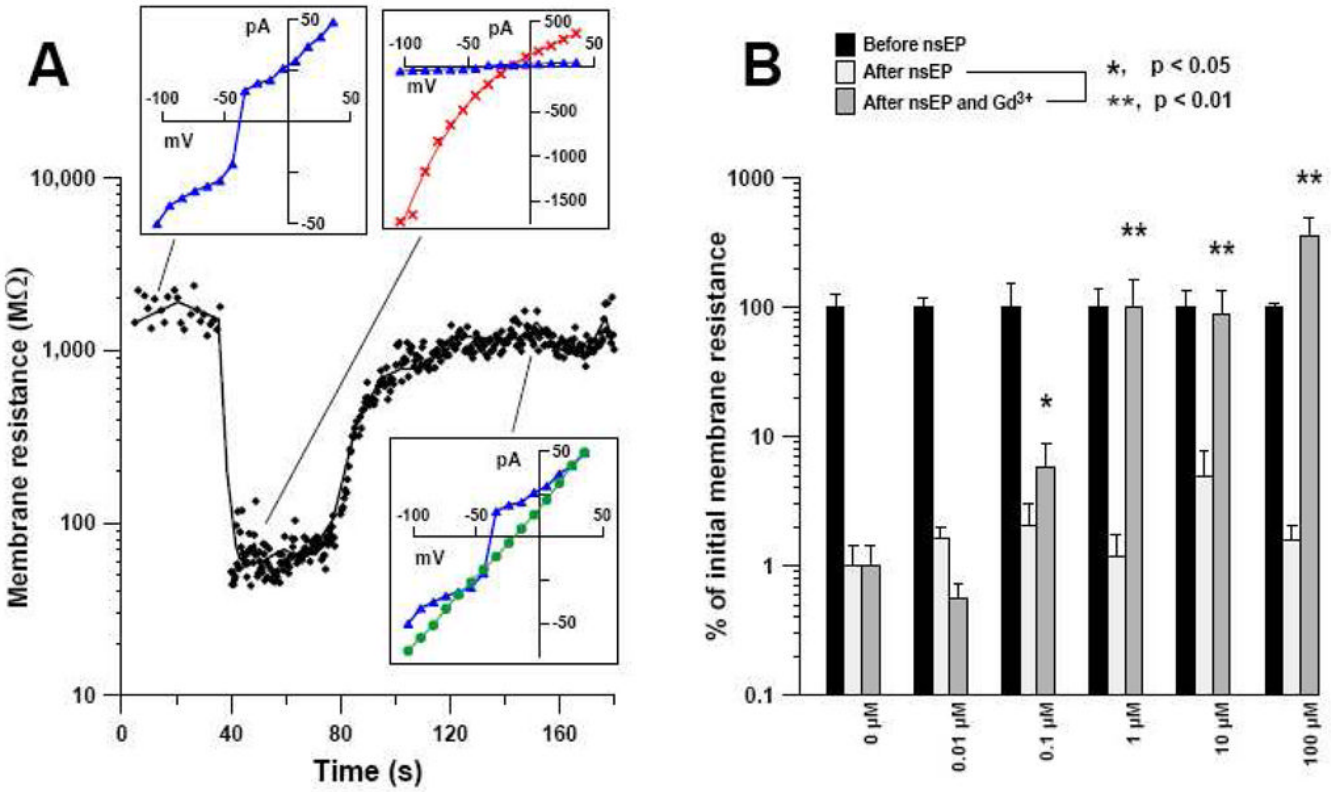

Fig. 1.

Restoration of plasma membrane electrical resistance (R_m) by Gd^{3+} in nsEP-exposed Jurkat cells (one 60 ns pulse at 8 kV/cm). (A) Example of R_m changes in response to nsEP (at 30 s) followed by perfusion with 1 μM of Gd^{3+} (at 80 s). Insets show representative *I–V* curves at different times. (B) Restoration of R_m by Gd^{3+} in nsEP-treated cells as a function of Gd^{3+} concentration. Shown are R_m values that were measured 30 s before nsEP exposure, 30 s after it, and after 50 s of perfusion with Gd^{3+}. The data have been normalized to pre-exposure Rm in individual cells. Shown are mean values ± s.e. (n= 3–4).

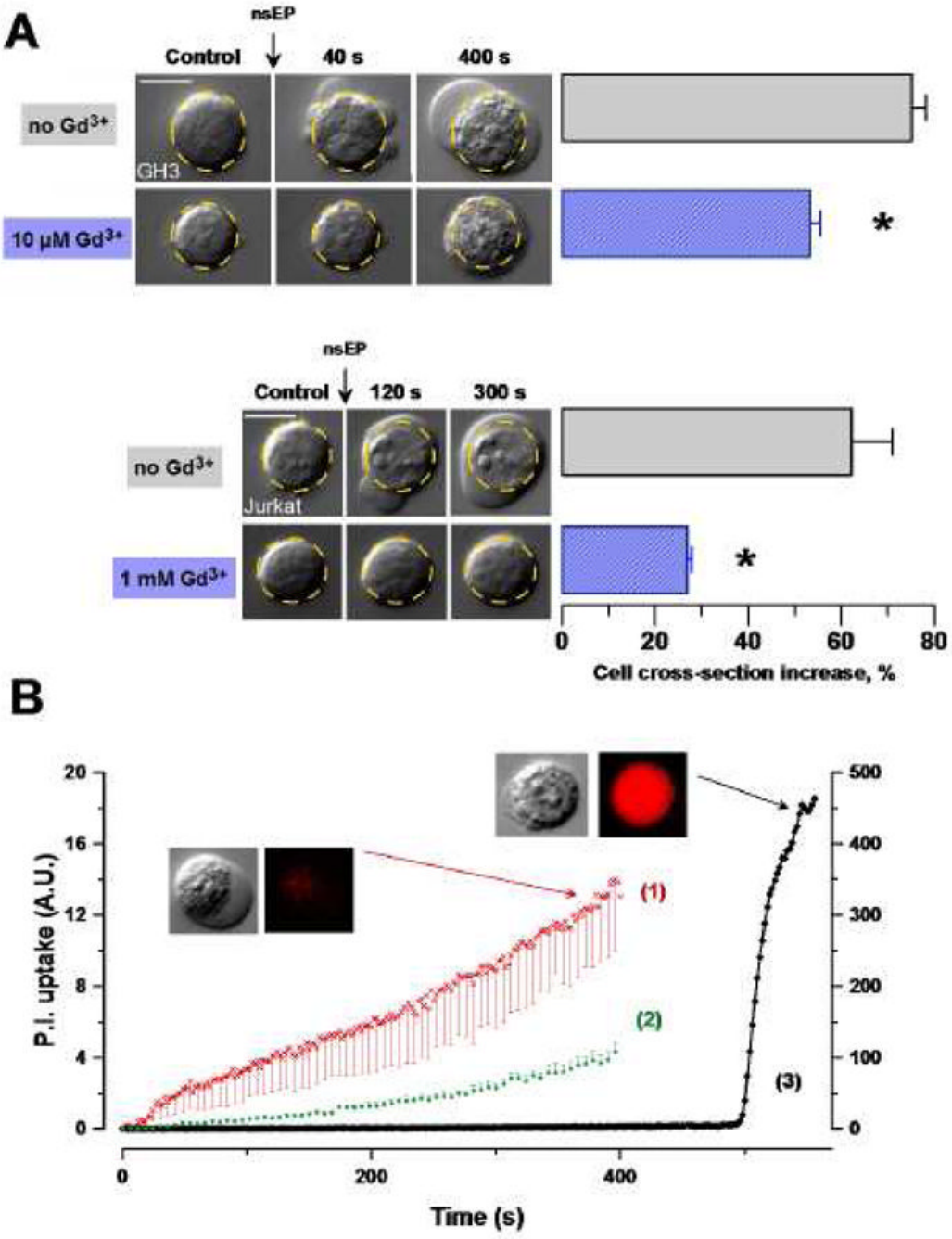

Fig. 2.

Gd^{3+} reduces nsEP-induced cell swelling and blebbing, and membrane permeabilization to propidium. (A) Representative images of morphological changes in Jurkat and GH3 cells exposed to nsEP (100 × 12kV/cm, 60ns, 2Hz and 20 × 12kV/cm, 600ns, 2Hz, respectively) with or without Gd^{3+} in the bath buffer. The dashed-line circle is a contour of the cell prior to exposure. Bar graphs display respective mean changes in the cell cross-section as seen on a DIC image (mean ± s.e., n=6 (control) and 9 (exposed) for GH3, and 3 and 5, respectively, for Jurkat; $p<0.01$ for Gd^{3+} effect in both cell lines). Calibration bars: 10 μm. (B), Propidium uptake in GH3 cells, (1) after nsEP (n=3), (2) after nsEP + 10 μM Gd^{3+} (n=4), (3) after permeabilization with 0.03% digitonin at 500 s (n=1). (1) and (2) use left Y-axis and (3) use

right Y-axis. nsEP conditions: 20 pulses at 2 Hz, 600 ns, 12 kV/cm, starting at 10 s. Shown are mean values ± s.e.; error bars are one-sided for clarity. Insets show typical DIC and propidium fluorescence images of nsEP- and digitonin-treated cells.

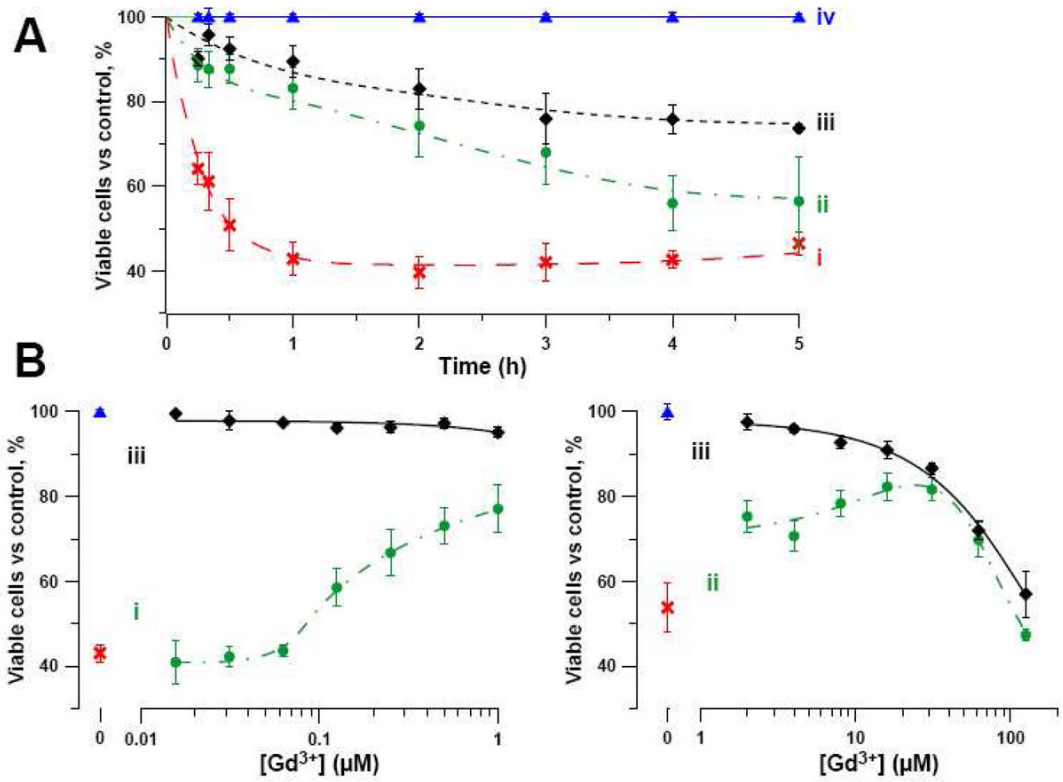

Fig. 3.

Gd^{3+} increases survival of nsEP exposed cells. For all panels, cell survival was measured by propidium exclusion by individual cells (Jurkat) using flow cytometry (10,000 cells per sample). Shown are mean ± s.e., n = 3–5. Survival level in control samples (sham exposure, no Gd^{3+}) for the respective time point was taken as 100%. (A): Changes in the viable cell fraction over time after treatment, (i) by nsEP, (ii) by nsEP + 30 μM Gd^{3+}, (iii) by 30 μM Gd^{3+}, (iv) by sham exposure (control). nsEP conditions: 10 × 60 ns at 20 kV/cm. (B): Effect of Gd^{3+} concentration in the bath buffer on cell survival measured 1 h after nsEP exposure with 30 pulses, 60 ns, 20 kV/cm (i) or 10 pulses, 60 ns, 20 kV/cm (ii) or sham exposure (iii).